3

COUPLED FINITE ELEMENT AND BOUNDARY ELEMENT METHODS IN ELECTROMAGNETIC SCATTERING

K. L. Wu, G. Y. Delisle, D. G. Fang and M. Lecours

3.1 Introduction
3.2 General Formulation
a. The Problem
b. Finite Element Method (FEM)
c. Boundary Element Method (BEM)
d. Combination of the FEM and BEM
3.3 Implementation and Numerical Results
3.4 Conclusion
Acknowledgements
References

3.1 Introduction

The problem of electromagnetic scattering by various objects has always been a subject of interest for researchers in various disciplines. Many analytical and numerical methods have been proposed in order to handle the numerous electromagnetic scattering situations. For example, numerical techniques are available [1–3] to solve the integral equation which arises in the formulation of the induced or polarized current on or inside objects of various shapes. These techniques, however, lead to very tedious computations when a complicated structure is involved as well as to numerical evaluations that are most impractical when dealing with multi-media problems. The unimoment method calls for a finite element representation of the field inside the object

while the scattered field is represented with an eigenfunction series expansion [4]. The boundary conditions, either physical or mathematical, are well-defined for a given boundary but only the circle appears to be a convenient computational choice in 2-D problems. Furthermore, in the original version of the unimoment method an inaccurate finite difference evaluation of the normal derivative of the numerical solution is used in the enforcement of continuity at the boundary with the normal derivative of the external cylindrical harmonic scattered field expansion.

More recently, the Boundary Element Method (BEM) [5] has been applied to electromagnetic scattering problems [6,7]. The main advantage of the BEM is the need to discretize only the boundary; in contrast, the Finite Element Method (FEM) considers the entire domain. Furthermore, it can easily take into account the radiation condition for unbounded situations such as scattering problems. A disadvantage of the BEM is that it leads to a fully populated system of equations, which is non-symmetric, in contrast with the sparsely populated and symmetric stiffness matrix obtained from the FEM. The BEM is usually restricted to homogeneous and isotropic problems because of the difficulty in seeking the needed fundamental solution for inhomogeneous and anisotropic problems. This weakness of the BEM does not encourage a search for the systematic solution to general problems with multi-media and anisotropic domains. The FEM is superior to the BEM in such cases, but it is difficult to introduce the radiation condition without increasing the requirements either in computer speed or storage capacity [9,10]. These facts suggest that a form of coupling between these two methods would be of great interest in many practical problems.

The main objective of this chapter is to present a combined FEM-BEM method that can be used to solve the scattering fields by an inhomogeneous arbitrary isotropic scatterer. This method can also be extended to handle the case of anisotropic materials with only slight modifications. In the proposed method, called coupled finite boundary element method (CFBM), an analytic relation between the field and its derivative on the boundary is used; no artificial boundary is needed. The importance of this feature is obvious when the scattering object is long and slender. Furthermore, the proposed method does not suffer from having non-unique solutions in the resonance case. We analyze several examples, and compare the results with those obtained by the BEM to validate our combined FEM-BEM method.

3.2 General Formulation

a. *The Problem*

To minimize the details, only the two-dimensional case is discussed. The domain of the problem is divided into two regions. One is the interior region R which includes the scatterer and is enclosed completely by the boundary, B, as shown in Fig. 1. B may be the physical boundary of the scatterer, but is not necessarily so. Another is the exterior region enclosed by B and the infinite boundary.

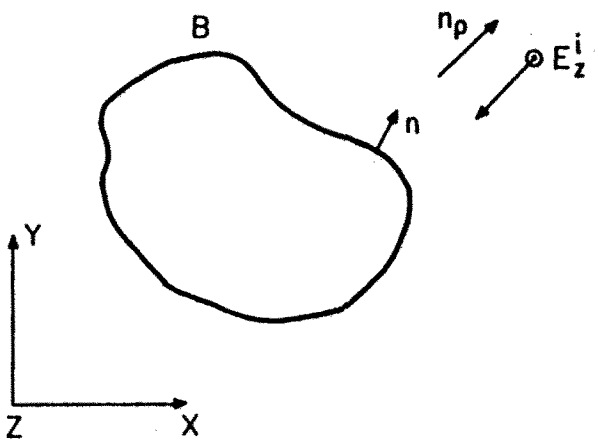

Figure 1 Two-dimensional dielectric scattering problem.

So the two-dimensional scattering problem can be treated mathematically as two separate problems. One can be considered as a closed boundary value problem which is described by the following differential equation (see Fig. 1)

$$(\nabla^2 + k^2)\, u' = 0 \quad \text{in } R \tag{1}$$

$$u' = \underline{u} \quad \text{on } B \tag{2}$$

$$q' = \underline{q} \quad \text{on } B \tag{3}$$

where q' is the outward normal derivative of $u', k = \sqrt{\epsilon_0 \epsilon_r \mu_0}$ and $\underline{u}, \underline{q}$ are known values.

The other can be regarded as an unbounded case and is expressed in integral equation form over the domain bounded by C, defined as the boundary B and the infinity as

$$u'(\bar{r}_f) = \int_C \left[\phi(\bar{r}_f|\bar{r}_o) \frac{\partial u(\bar{r}_o)}{\partial n'} - u(\bar{r}_o) \frac{\partial \phi(\bar{r}_f|\bar{r}_o)}{\partial n'} \right] d\Gamma + u^i(\bar{r}_f) \tag{4}$$

where $u^i(\bar{r})$ and $u(\bar{r})$ are the incident and the scattered fields respectively, $u(\bar{r})$ satisfies the radiation condition, $\hat{n}'$ is an outward unit vector normal to the boundary C of outside region, $\bar{r}_f$ is an arbitrary field point and $\bar{r}_o$ is a point on the boundary.

In (4), the fundamental solution

$$\phi(\bar{r}_f|\bar{r}_o) = -\frac{j}{4} H_0^{(2)}(k|\bar{r}_f - \bar{r}_o|) \tag{5}$$

is introduced, where $H_0^{(2)}(\cdot)$ is the Hankel function of the second kind and zero order.

b. *Finite Element Method (FEM)*

With the finite element approach, the primary dependent variables are replaced by a system of discretized variables over the domain under consideration. Therefore, the domain itself is discretized into finite elements which are connected at the nodals. The compatibility within the element and between element boundaries is ensured by the choice of the shape function. In the present analysis, the region R is discretized into a number of second order triangular elements as shown in Fig. 2.

Within an arbitrary shaped triangle, the field value u is written in terms of second-order complete polynomials as

$$u = \{N\}^T \{u\}_e \tag{6}$$

where

$$\{N\} = [N_1, N_2, N_3, N_4, N_5, N_6]^T \tag{7a}$$

and

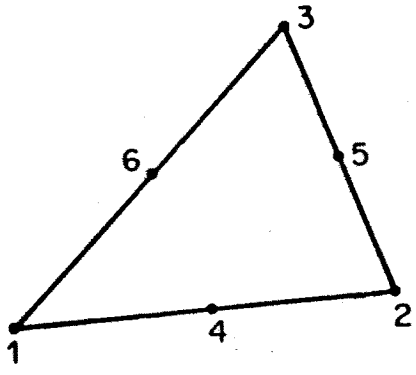

Figure 2 Second-order triangular element.

$$\{u_i\}_e = [u_1, u_2, u_3, u_4, u_5, u_6]_e^T \tag{7b}$$

u_i being the field at the ith nodal point of the element. Column vectors are denoted by $\{\cdot\}$ while $\{\cdot\}^T$ represents a row vector where a T superscript denotes transpose. The shape functions N_1 through N_6 are given by

$$N_1 = L_1(2L_1 - 1) \tag{8a}$$

$$N_2 = L_2(2L_2 - 1) \tag{8b}$$

$$N_3 = L_3(2L_3 - 1) \tag{8c}$$

$$N_4 = 4L_1L_2 \tag{8d}$$

$$N_5 = 4L_2L_3 \tag{8e}$$

$$N_6 = 4L_1L_3 \tag{8f}$$

where L_1, L_2 and L_3 are the area coordinates in the finite element

approach. Substituting (6) into (1) and using a Galerkin procedure, after integrating by parts, results in

$$\begin{bmatrix} [A_{RR}] & [A_{RB}] \\ [A_{BR}] & [A_{BB}] \end{bmatrix} \begin{Bmatrix} \{u'\}_R \\ \{u'\}_B \end{Bmatrix} = \begin{Bmatrix} \{0\} \\ [B_B] \left\{ \dfrac{\partial u'}{\partial n} \right\}_B \end{Bmatrix} \tag{9}$$

where the matrix on the left hand side can be computed by using

$$\begin{bmatrix} [A_{RR}] & [A_{RB}] \\ [A_{BR}] & [A_{BB}] \end{bmatrix} = \sum_e \iint \Big[\frac{\partial \{N\}}{\partial x} \cdot \frac{\partial \{N\}^T}{\partial x} + \frac{\partial \{N\}}{\partial y} \cdot \frac{\partial \{N\}^T}{\partial y}$$

$$- \epsilon_r (1 - \jmath \tan \delta) k_0^2 \{N\}\{N\}^T \Big] \, dx \, dy \tag{10}$$

and

$$[B_B] = \sum_e{}' \int_e \{N\}\{N\}^T \, d\Gamma \tag{11}$$

In these equations, $k_0 = \omega^2 \epsilon_0 \mu_0$ and $\tan \delta$ is the loss tangent. The integral in (10) can be calculated analytically, and for a second order finite element, (11) can be expressed as

$$[B_B] = \sum_e{}' \frac{l_e}{15} \begin{bmatrix} 2 & 1 & -0.5 \\ 1 & 8 & 1 \\ -0.5 & 1 & 2 \end{bmatrix} \tag{12}$$

The components of $\{u'\}_R$ correspond to the nodal values in R and $\{u'\}_B$ on B, $\sum_e$ and $\sum_e'$ extend over all the different elements and elements related to boundary B respectively. The l_e is the length of e-th boundary element. Equation (9) is the FEM matrix equation.

c. Boundary Element Method (BEM)

The region under consideration for the exterior problem is enclosed by boundary B and a boundary at infinity. Because the radiation condition cannot be applied for the incident wave, the scattering wave should vanish at infinity. Equation (4) is then rewritten as

$$u(\bar{r}_f) = \int_B \left[\phi(\bar{r}_f|\bar{r}_o)\frac{\partial u(\bar{r}_o)}{\partial n'} - u(\bar{r}_o)\frac{\partial \phi(\bar{r}_f|\bar{r}_o)}{\partial n'}\right] d\Gamma \tag{13}$$

$$u'(\bar{r}_f) = u(\bar{r}_f) + u^i(\bar{r}_f) \tag{14}$$

If field point $\bar{r}_f$ is placed on the boundary B, a singularity will occur. To extract the contribution of the singularity, the integration path ΔB going around the point $\bar{r}_f$ is considered. Denoting $\partial u/\partial n'$ as q, (13) is rewritten as follows

$$u(\bar{r}_f) = \left[\lim_{\epsilon\to 0}\int_{B'} q\phi\, d\Gamma + \lim_{\epsilon\to 0}\int_{\Delta B} q\phi\, d\Gamma\right]$$

$$-\left[\lim_{\epsilon\to 0}\int_{B'} u\frac{\partial\phi}{\partial n'}\, d\Gamma + \lim_{\epsilon\to 0}\int_{\Delta B} u\frac{\partial\phi}{\partial n'}\, d\Gamma\right] \tag{15}$$

The integrations over the boundary ΔB can be estimated by using the small argument asymptotic expression of the Hankel function

$$\begin{aligned}\lim_{\epsilon\to 0}\int_{\Delta B} u\frac{\partial\phi}{\partial n'}\, d\Gamma &= \lim_{\epsilon\to 0}\int_{\Delta B} u\frac{\jmath}{4}kH_1^{(2)}(k\epsilon)\, d\Gamma \\ &= u\frac{\jmath}{4}kH_1^{(2)}(k\epsilon)\epsilon\theta \\ &= \frac{\jmath}{4}k\theta u\lim_{\epsilon\to 0}\left[\epsilon\left\{\frac{k\epsilon}{2} - \jmath\left(\frac{2}{\pi}\frac{1}{k\epsilon}\right)\right\}\right] \\ &= \frac{\theta}{2\pi}u(\bar{r}_f)\end{aligned} \tag{16}$$

$$\lim_{\epsilon \to 0} \int_{\Delta B} q\phi \, d\Gamma = \lim_{\epsilon \to 0} \int_{\Delta B} q\{\tfrac{\jmath}{4} H_0^{(2)}(k\epsilon)\} \, d\Gamma$$

$$= \lim_{\epsilon \to 0} \left[\frac{-\jmath}{4} q \left\{ 1 - \jmath \frac{2}{\pi} (ln(k\epsilon) + \gamma - ln2) \right\} \epsilon\theta \right]$$

$$= 0 \tag{17}$$

This then yields

$$(1 - \frac{\theta}{2\pi}) u_i(\bar{r}_f) + \int_B \frac{\partial \phi(\bar{r}_f | \bar{r}_0)}{\partial n'} u(\bar{r}_0) \, d\Gamma$$

$$= \int_B \phi(\bar{r}_f | \bar{r}_0) \frac{\partial u(\bar{r}_0)}{\partial n'} \, d\Gamma \tag{18}$$

with

$$\int_B = \lim_{\epsilon \to 0} \int_{B'}$$

where a Cauchy's principal value of integration is assumed in this case.

An approximate solution to (18) can be obtained by discretizing the boundary into the so-called boundary elements. These elements are similar to finite elements except that their dimensions are usually one less than the dimensions of the problem. For the present analysis, second-order boundary elements are used for the sake of compatibility with the second-order finite elements (Fig. 3).

Within each elements, u and q are defined respectively in terms of u_l and q_l at the three nodal points, $l = 1, 2, 3$, by using

$$u = \{M\}^T \{u\}_e \tag{19a}$$

$$q = \{M\}^T \{q\}_e \tag{19b}$$

where

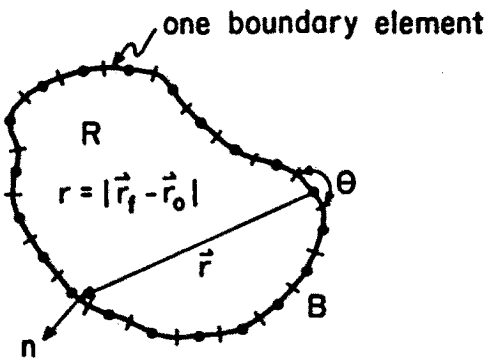

Figure 3 Integration on each boundary element.

$$\{u\}_e = [u_1, u_2, u_3]^T \tag{20a}$$

$$\{q\}_e = [q_1, q_2, q_3]^T \tag{20b}$$

$$\{M\} = [M_1, M_2, M_3]^T \tag{20c}$$

The boundary element shape function, M_l, is given by

$$M_l = A_l \xi^2 + B_l \xi + C_l \tag{21}$$

where

$$A_1 = 1/2,\ A_2 = 1/2,\ A_3 = -1$$

$$B_1 = -1/2,\ B_2 = 1/2,\ B_3 = 0$$

and

$$C_1 = 0,\ C_2 = 0,\ C_3 = 1$$

When the normalized coordinate, ξ, is defined on the e-th boundary element, it can be easily checked that M_1, M_2, M_3 are equal to

the finite element shape functions evaluated on the boundary. This characteristic aids in making the coupling of the FEM and the BEM accurate.

Substituting (9a),(9b) into (18), we obtain

$$\left[1-\frac{\theta}{2\pi}\right]u_i+\sum_{e=1}^{N}[h_1,h_2,h_3]_e\begin{Bmatrix}u_1\\u_2\\u_3\end{Bmatrix}=\sum_{e=1}^{N}[g_1,g_2,g_3]_e\begin{Bmatrix}q_1\\q_2\\q_3\end{Bmatrix} \tag{22}$$

When the nodal point i does not belong to the e-th element, h_l and g_l can be calculated with Gaussian integration as

$$h_l=\frac{L}{2}\int_{-1}^{1}M_l\frac{\partial\phi(\bar{r}_f|\bar{r}_o)}{\partial n'}\,d\xi \tag{23}$$

$$g_l=\frac{l}{2}\int_{-1}^{1}M_l\phi(\bar{r}_f|\bar{r}_o)\,d\xi \tag{24}$$

where L is the length of the element. When the nodal point i belongs to the e-th element, considering the limit of $\epsilon\to 0$, we can get

$$h_l=0 \tag{25}$$

and if the nodal point, i, coincides with the nodal point $l=1$, 2, or 3, g_l is given by [8]

$$g_l=(\frac{L}{2})[A_lI_2(2)-(2A_l-B_l)\{I_1(2)-2/(\pi k^2L^2)\}$$
$$+(A_l-B_l+C_l)\,I_0\,(2)] \tag{26a}$$

$$g_l=(\frac{L}{2})[A_lI_2(2)-(2A_l+B_l)\{I_1(2)-2/(\pi k^2L^2)\}$$
$$+(A_l+B_l+C_l)\,I_0\,(2)] \tag{26b}$$

$$g_l=L[A_lI_2(1)+C_lI_0(1)] \tag{26c}$$

respectively. Here I_0, I_1, and I_2 are calculated as follows:

$$I_0(\eta) = \int \frac{1}{4\jmath} H_0^{(2)}\left[\frac{kL}{2}\eta\right] d\eta = -\frac{\eta}{4}\sum_{v=0}^{\infty} \frac{(-1)^v}{(2v+1)(v!)^2}\left[\frac{kL}{4}\eta\right]^{2v}$$
$$\cdot\left[\frac{2}{\pi}\left\{\gamma + ln\left[\frac{kL}{4}\eta\right] - \frac{1}{2v+1} - \sum_{s=1}^{v}\frac{1}{s}\right\} + \jmath\right] \tag{27a}$$

$$I_1(\eta) = \int \frac{\eta}{4\jmath} H_0^{(2)}\left[\frac{kL}{2}\eta\right] d\eta = \frac{1}{4\jmath}\frac{2\eta}{kL} H_1^{(2)}\left[\frac{kL}{2}\eta\right] \tag{27b}$$

$$I_2(\eta) = \int \frac{\eta^2}{4\jmath} H_0^{(2)}\left[\frac{kL}{2}\eta\right] d\eta \tag{27c}$$
$$= \left[\frac{2}{kL}\right]^2\left[\frac{kL}{2}\frac{\eta^2}{4\jmath} H_1^{(2)}\left[\frac{kL}{2}\eta\right] + \frac{\eta}{4\jmath} H_0^{(2)}\left[\frac{kL}{2}\eta\right] - I_0(\eta)\right]$$

where $\gamma = 0.57721...$ is Euler's constant. In matrix notation, (22) can be written as

$$\left[H_0\right]\left\{u\right\}_B = \left[G_0\right]\left\{q\right\}_B \tag{28}$$

This BEM matrix equation is to be used later on.

d. *Combination of the FEM with BEM*

Since the fundamental solution that is chosen for the BEM equation in the exterior region satisfies the radiation condition, it is not necessary to deal with the boundary at infinity. The FEM cannot, however, easily take into account this radiation condition. On the other hand, it is superior to the BEM in handling multi-media problems. In the proposed method, the BEM is therefore used for the region outside the boundary B, which may be the actual boundary of the obstacle, or any artificial geometrical boundary set up for the convenience of treating multi-media problems; fields inside of B are treated by the

FEM, with the interior and exterior problems being separately solved first and these solutions being subsequently coupled.

Figure 2 shows a second order finite element. Both boundary element and finite element are connected on the interface B. To ensure a correct coupling of boundary and finite elements at the interface, conditions of compatibility and equilibrium must be satisfied. The compatibility condition can be reached if both elements have common nodals at the interface and if the shape functions describing the field variation at the interface are identical for the BEM and the FEM. The equilibrium is satisfied when the field normal derivatives at the nodal point of the boundary element mesh are equal and opposite to that of the finite element mesh at the interface. So, on the boundary B, the following boundary conditions must be satisfied

$$\{u'\}_B = \{u\}_B + \{u^i\}_B \tag{29}$$

$$-V^I\left(\{\frac{\partial u'}{\partial n}\}_B\right) = V^{II}\left(\{\frac{\partial u}{\partial n'}\}_B + \{\frac{\partial u^i}{\partial n'}\}_B\right) \tag{30}$$

$$u = \begin{cases} E_z & \text{for TM case} \\ H_z & \text{for TE case} \end{cases} \tag{31}$$

$$V^I = \begin{cases} 1.0 & \text{for TM case} \\ \dfrac{1}{\epsilon_{r_I}} & \text{for TE case} \end{cases} \tag{32}$$

$$V^{II} = \begin{cases} 1.0 & \text{for TM case} \\ \dfrac{1}{\epsilon_{r_{II}}} & \text{for TE case} \end{cases} \tag{33}$$

where ϵ_{r_I} and $\epsilon_{r_{II}}$ are the relative permittivities of the interior and the exterior, respectively. In addition, the incident wave is expressed as follows

$$u^i = u_0 \exp(jk|\overline{\rho}|) \tag{34}$$

The coordinate $\overline{\rho}$ is chosen in the direction of the incident wave and it is easy to obtain

$$q^i = \frac{\partial u^i}{\partial n} = -\jmath k \hat{n} \cdot \hat{n}_\rho \, u^i \tag{35}$$

which can be expressed as

$$\{q^i\}_B = [D]\{u^i\}_B \tag{36}$$

where $[D]$ is a diagonal coefficient matrix.

Equations (29) and (30) form the bridge between the two different regions. This bridge connects FEM equation (9) with BEM equation (28). By substituting (29), (30), and (36) into (9) and merging (9) and (28) into one matrix relationship, the following is obtained for both interior and exterior regions

$$\begin{bmatrix} [A_{RR}] & [A_{RB}] & [0] \\ [A_{BR}] & [A_{BB}] & -[B_B] \\ [0] & [H_0] & [G_0] \end{bmatrix} \begin{Bmatrix} \{u\}_R \\ \{u^s\}_B \\ \{q^s\}_B \end{Bmatrix} = \begin{Bmatrix} -[A_{RB}]\{u^i\}_B \\ ([B_B][D] - [A_{BB}])\{u^i\}_B \\ \{0\} \end{Bmatrix} \tag{37}$$

With the help of (37), the scattered field and its normal derivative on the boundary B can be obtained provided that the incident wave is given. These quantities correspond to surface electric and magnetic sources. Generally we are interested in observable quantities in the far field, the solution of the final matrix equation (37) being merely an intermediate step. In the following, the results of the scattered fields are given. With the scattered fields, the radar cross section is easily obtained.

Using the asymptotic expression of the Hankel function, the far field pattern can be found by a modification of (16) as follows

$$E_z\Big|_{r\to\infty} = A \left[\sum_{e=1}^{N} [g_1', g_2', g_3']_e \begin{Bmatrix} q_1^s \\ q_2^s \\ q_3^s \end{Bmatrix}_e - \sum_{e=1}^{N} [h_1', h_2', h_3']_e \begin{Bmatrix} u_1^s \\ u_2^s \\ u_3^s \end{Bmatrix}_e \right] \tag{38}$$

with

$$h_1' = jk \int_{-1}^{1} (\frac{1}{2}\xi_2 - \frac{1}{2}\xi) \cos(\overline{r}, \widehat{n})\, e^{-jk\Delta r}\, d\xi \tag{39}$$

$$h_2' = jk \int_{-1}^{1} (\frac{1}{2}\xi_2 + \frac{1}{2}\xi) \cos(\overline{r}, \widehat{n})\, e^{-jk\Delta r}\, d\xi \tag{40}$$

$$h_3' = jk \int_{-1}^{1} (-\xi_2 + 1) \cos(\overline{r}, \widehat{n})\, e^{-jk\Delta r}\, d\xi \tag{41}$$

$$g_1' = \int_{-1}^{1} (\frac{1}{2}\xi_2 - \frac{1}{2}\xi)\, e^{-jk\Delta r} d\xi \tag{42}$$

$$g_2' = \int_{-1}^{1} (\frac{1}{2}\xi_2 + \frac{1}{2}\xi)\, e^{-jk\Delta r} d\xi \tag{43}$$

$$g_3' = -\int_{-1}^{1} (-\xi_2 + 1)\, e^{jk\Delta r} d\xi \tag{44}$$

where Δr is the relative distance difference over the incoming wavefront and A is a constant amplitude.

Equation (38) is the expression sought-after for the scattered far field in terms of the surface electric and magnetic currents when the BEM is used for the outer region.

3.3 Implementation and Numerical Results

To show the validity and the implementation of the combined method, several examples are discussed. The procedure of solving a given problem using CFBM may be divided into three basic steps. First, it is necessary to choose a boundary B. The rule of thumb is to enclose the scatterer completely and let the interior domain be as small as possible in order to minimize the number of unknowns in the FEM mesh. If the near field distribution is required, the boundary B can be extended as far as needed, but at the expense of the computational effort. The second step in the solution development involves dividing the interior region into finite elements. Each element should be homogeneous; otherwise the inhomogeneous element technique must be used by slightly modifying equation (10). In fact, boundary elements are

formed sequentially after finite element generation because boundary elements are just the finite elements on the boundary B. It should be noted that nodal numbering must be such that the boundary nodes of the interior region are identical to those of the exterior region. The final step in solving the problem is to fill in the matrix equation as described in section 2 and to solve it.

As a first example, a layered dielectric square cylinder is investigated ($\epsilon_1 = 2.89$, $\epsilon_2 = 1.0$, $\epsilon_3 = 2.89$) and the results are shown in Fig. 4 in dotted line. A dielectric hollow square cylinder is also analyzed with the same program and the results are plotted using a solid line on Fig. 4. It agrees well with the BEM solution of Yashiro and Ohkawa [7] which is superposed on our solution with triangular points for comparison purposes.

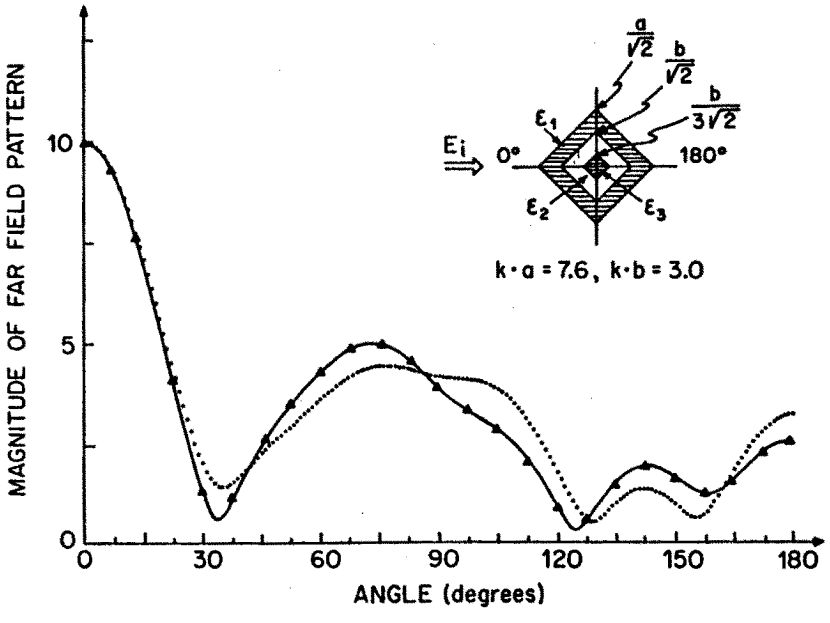

Figure 4 Far-field pattern for layered-square cylinders:
··· CFBM result for layered square cylinder ($\epsilon_1 = \epsilon_3 = 2.89$, $\epsilon_2 = 1.0$)
— CFBM result for hollow square cylinder
▲▲ BEM result for hollow square cylinder ($\epsilon_1 = 2.89$, $\epsilon_2 = \epsilon_3 = 1.0$).

The second example is the scattering by the composite structure of a multi-dielectric cylinder ($\epsilon_1 = \epsilon_3 = 1.0$, $\epsilon_2 = 2.89$), as shown in

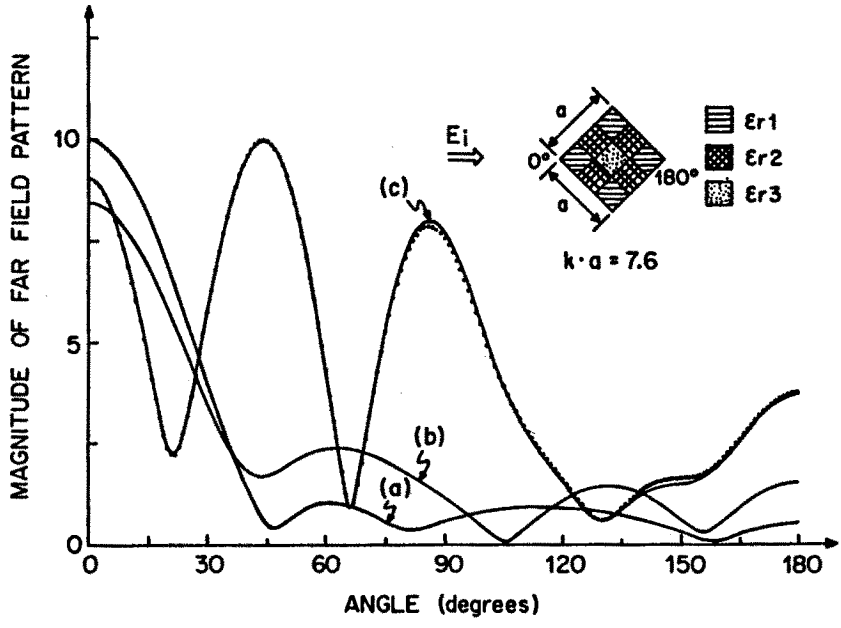

Figure 5 Far-field pattern for composite cylinders:
(a) — CFBM for composite cylinder ($\epsilon_1 = \epsilon_3 = 1.0$, $\epsilon_2 = 2.89$)
(b) — CFBM for cross dielectric cylinder ($\epsilon_1 = 1.0$, $\epsilon_2 = \epsilon_3 = 2.89$)
(c) — CFBM for dielectric square cylinder with $\epsilon_r = 2.89$
··· BEM solution for the dielectric square cylinder.

Fig. 5 (solid line (a)). Two special cases are also considered: one is the cross-dielectric cylinder ($\epsilon_1 = 1.0, \epsilon_2 = \epsilon_3 = 2.89$) (solid line (b)), the other is the dielectric square cylinder ($\epsilon_1 = \epsilon_2 = \epsilon_3 = 2.89$) (solid line (c)). The BEM result for the square cylinder case is also given (dotted line) for the purpose of checking the validity of our method.

Figure 6 shows the far field pattern corresponding to a perfectly conducting circular cylinder with dielectric periodic load. In this example, only the dielectric coated ring domain needs to be treated as the interior region. It should be noticed that the change of ϵ_r may cause large differences in the far field pattern. A comparison of the analytic solution and the CFBM solution at the resonant frequency [7] for the scattering of a perfectly conducting circular cylinder can be obtained by setting the ϵ_r of dielectric coating equal to 1.0 . There are excellent agreements between these two solutions, both for TM and TE cases. This demonstrates that the proposed method does not suffer from the

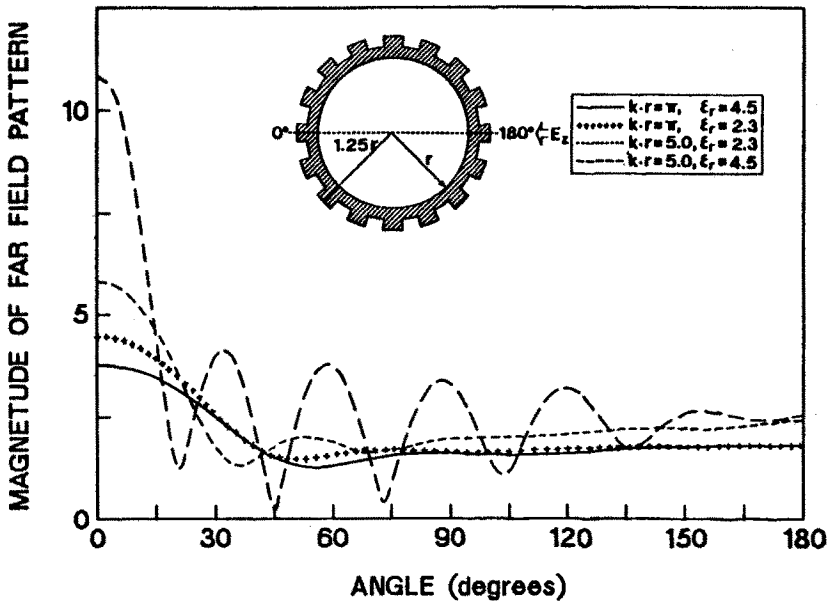

Figure 6 Far-field pattern for a perfectly conducting circular cylinder with dielectric periodic load.

non-uniqueness problem in the resonance case as the BEM does. The reason is that the BEM only involves an electric field integral equation which suffers from non-uniqueness. However, in the CFBM, the integral equation is complemented by a differential equation which is satisfied in the interior region.

The last numerical example is radio wave propagation in a building. To see the near field distribution around the building, the model of the structure is enclosed with an artificial boundary B as shown in Fig. 7. Because the thickness of the wall is much smaller than the dimension of the building, inhomogeneous finite elements are used where needed.

In all the cases considered above, the incident plane wave is TM polarized, although the mathematical treatment is generally applicable for both TE and TM cases. The method proposed here can be extended to cover some anisotropic cases. If the anisotropy involves coupling between x and y directions, the above treatment needs only slight modifications. In this chapter, only the case of an exterior source to

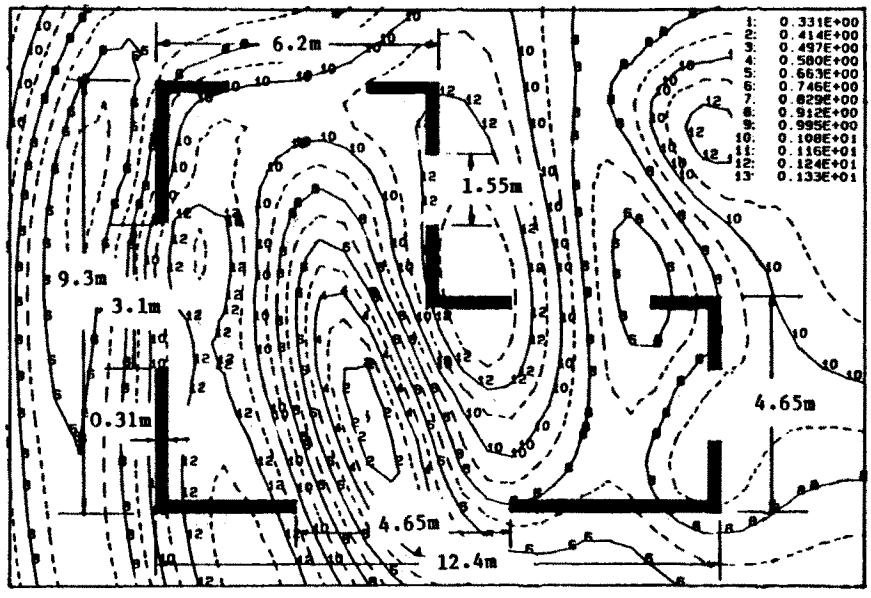

Figure 7 Equal level of normalized electric field distribution in a typical building. Dimensions of the building model are indicated in meters. The walls have assumed ϵ_r =5.0-j1.0 and k_0 =0.5 radians/meter.

the cylinder has been considered. The internal source case can be developed using an analogous procedure.

3.4 Conclusion

It has been shown that the finite element and boundary element methods can be coupled together to study difficult electromagnetic scattering problems. This new procedure, known as the Coupled Finite-element Boundary-element Method (CFBM), is a unified numerical approach that can handle inhomogeneous arbitrary scatterers efficiently.

The method may be used in many situations where the evaluation of scattering by a complex dielectric object or the analysis of a coated structure is involved. But, for the case of homogeneous scatterers, the method loses its advantage and other numerical methods such as the moment method or BEM can be adopted.

In problems where the size of the resultant finite element matrix is much larger than that of the boundary element matrix, an appropriate treatment of the sparse matrix can save a great deal of computer time. This requires much less memory space to handle the full problem while still yielding a valid solution. The extension of the method to three dimensional scattering problems, including cases where the sources are internal to the scattering object is possible. This method may also be combined with the spectral domain technique to treat more complicated problems, for example, to solve the scattering problem of certain objects above or within a multi-layered medium by using the corresponding spatial Green's function which has been recently developed [11].

Acknowledgements

This research was financed by the Natural Sciences and Engineering Council, Ottawa, Canada, K1A 1H5.

References

[1] Harrington, R. F., *Field Computation by Moment Methods*, New York Macmillan, 1968.

[2] Okamoto, N., "Matrix formulation of scattering by a homogeneous gyrotropic cylinder," *IEEE Trans. Antennas Propagat.*, **AP-18**, 642–649, 1970.

[3] Richmond, J. H., "Scattering by dielectric cylinder of arbitrary cross section shape," *IEEE Trans. Antennas Propagat.*, **AP-13**, 334–341, 1965.

[4] Chang, S. K., and K. K. Mei, "Application of the unimoment method to electromagnetic scattering of dielectric cylinders," *IEEE Trans. Antennas Propagat.*, **AP-24**, 35–42, 1976.

[5] Brebbia, C. A., and S. Walker, *Boundary Element Techniques in Engineering*, Newnes-Butterworths, London, 1980.

[6] Kagami, S., and I. Fukou, "Application of boundary-element method to electromagnetic field problems," *IEEE Trans. Microwave Theory Tech.*, **MTT-32**, 455–461, 1984.

[7] Yaskiro, K. I., and S. Ohkawa, "Boundary element method for electromagnetic scattering from cylinders," *IEEE Trans. Antennas Propagat.*, **AP-23**, 383–389, April 1985.

[8] Koshiba, M., and M. Suzuki, "Application of the boundary-element method to waveguide discontinuities," *IEEE Trans. Microwave Theory Tech.*, **MTT-34**, 301–307, 1986.

[9] Silvester, P., and M. S. Hsich, "Finite-element solution of two-dimensional exterior field problems," *Proc. Inst. Elec. Eng.*, **118**, 1743–1747, 1971 .

[10] McDonald, B. H., and A. Wexler, "Finite-element solution of unbounded field problems," *IEEE Trans. Microwave Theory Tech.*, **MTT-20**, 841–847, 1972 .

[11] Fang, D. G., J. J. Yang, and G. Y. Delisle, "The discrete exact image theory for arbitrarily oriented dipoles in a multilayered medium," accepted for publication in *IEE Proc. Pt.H, Microwave, Antennas and Propagation.*